© 2017. Published by The Company of Biologists Ltd | Journal of Cell Science (2017) 130, 3360-3373 doi:10.1242/jcs.196642

RESEARCH ARTICLE

BCAP is a centriolar satellite protein and inhibitor of ciliogenesis

Paul de Saram*, Anila Iqbal*, Jennifer N. Murdoch and Christopher J. Wilkinson‡

ABSTRACT

The centrosome and cilium are organelles with important roles in microtubule organisation, cell division, cell signalling, embryogenesis and tissue homeostasis. The two organelles are mutually exclusive. The centriole/basal body is found at the core of the centrosome (centriole) or at the base of the cilium (basal body) and to change which organelle is present in a cell requires modification to the centriole/basal body both in terms of composition and sub-cellular localisation. While many protein components required for centrosome and cilium biogenesis have been described, there are far fewer known inhibitors of ciliogenesis. Here, we show that a protein called BCAP and labelled in the sequence databases as ODF2-like (ODF2L) is a ciliation inhibitor. We show that it is a centriolar satellite protein. Furthermore, our data suggest that BCAP exists as two isoforms with subtly different roles in inhibition of ciliogenesis. Both are required to prevent ciliogenesis and one additionally controls cilium length after ciliogenesis has completed.

KEY WORDS: Centriolar satellite, Cilia, Centrosome, ODF2L

INTRODUCTION

Cilia are hair-like structures found on the surface of many cell types that have important roles in cell signalling and embryogenesis (Nigg and Raff, 2009). Cilium defects cause inherited diseases (Badano et al., 2006), polycystic kidney disease being the most prevalent (Ong and Wheatley, 2003). Knowledge of the roles and component parts of the cilium has greatly expanded in the last decade. However, control of when a cell makes a cilium is still poorly understood.

The cilium acts as a 'mast' or antenna for many signalling pathways, including hedgehog signalling (Huangfu et al., 2003). Mutations in various cilium components give rise to a large number of individual, mainly rare, diseases that are grouped together as the ciliopathies (Badano et al., 2006), including Meckel-Grubel, Alstrom, Joubert and Bardet-Biedl syndromes (Ansley et al., 2003; Collin et al., 2002; Dawe et al., 2007). These diseases affect multiple tissues and symptoms, include retinal degeneration, polydactyly, kidney cysts and neurological features, and reflect the multiple roles of cilia in cellular communication, cellular functioning and developmental biology.

The internal frame or superstructure of the cilium is composed of an axoneme of nine microtubule doublets, cylindrically arranged (Satir and Christensen, 2007). At the base of this is another microtubule-based structure, the barrel-shaped basal body. This closely resembles the centrioles found in the centrosome, the main microtubule-nucleating centre of animal cells and component of the two poles of the mitotic spindle (Bornens, 2002; Doxsey, 2001; Tassin and Bornens, 1999). Indeed, cells use a centriole to make the basal body and do so when they leave the cell cycle, either temporarily or when they differentiate into specialised cell types (Nigg and Raff, 2009).

The sequence of changes from centriole to basal body was first visualised by Sorokin using electron microscopy (Sorokin, 1962). One of the two centrioles, the mother centriole, which has additional, bracket-like appendage structures at its distal end, acquires a vesicle-like structure at this end and migrates to the cell surface. There the membranes fuse. The basal body is tightly bound to the membrane and transition zone fibres form between the two. The axoneme is templated from the basal body and extends, covered in membrane, away from the basal body.

The switch between centriole and basal body, centrosome and cilium is tightly regulated. Autophagy is used to remove molecules that otherwise inhibit ciliogenesis (Pampliega et al., 2013; Tang et al., 2013). Few negative regulators or inhibitors of ciliogenesis are known (Kim et al., 2010). Some are components of regulatory networks that affect processes in addition to ciliogenesis (Kim et al., 2010; Kasahara et al., 2014). Others, such as OFD1 and CP110, are centrosome components (Tang et al., 2013; Tsang et al., 2008). CP110 acts through Rab8 and Cep290 to inhibit ciliogenesis (Tsang et al., 2008). It also functions to prevent microtubules extending from the distal end of the centriole/basal body (Schmidt et al., 2009). It, therefore, also has a role in regulating centriole and centrosome duplication during S phase of the cell cycle, when two new centrioles bud from a template assembled on the side of the two existing centrioles and gradually extend until they reach full length in early G2. OFD1, similarly, is involved in regulating centriolar length and is also involved in distal appendage formation (Singla et al., 2010).

The centrosome components that are known to be negative regulators of ciliogenesis also have other roles in centrosome biology and centrosome/centriole duplication during the cell cycle. This, together with the necessarily tight control of whether a cell has a cilium versus a centrosome, suggests that dedicated, centrosome-localised inhibitors of ciliogenesis exist. Here, we report that BCAP is a negative regulator or inhibitor of ciliogenesis that needs to be removed for cilia to be made.

BCAP was first discovered by Ponsard and colleagues (Ponsard et al., 2007) but has since been annotated in the sequence databases as ODF2L or ODF2-like due to homology (28% identity, 51% similarity) to ODF2, a centriolar appendage protein (Lange and Gull, 1995; Nakagawa et al., 2001). Ponsard et al. found this protein to be expressed mainly in tissues containing motile cilia, where its expression increased as cells differentiated and ciliated. Five isoforms have been described, three long isoforms of ~65 kDa, and two short isoforms of 40 kDa. Ponsard et al. decribed BCAP as localising to basal bodies in ciliated cells and the centrioles of proliferating cells. Although there is similarity at the sequence level to ODF2, they observed that BCAP occupied a distinct zone within the centrosome.

Centre for Biomedical Sciences, Royal Holloway University of London, Egham, Surrey, TW20 0EX, UK.
*These authors contributed equally to this work

‡Author for correspondence (Christopher.Wilkinson@rhul.ac.uk)

C.J.W., 0000-0002-7448-0938

Received 12 August 2016; Accepted 31 July 2017

Journal of Cell Science (2017) 130, 3360-3373 doi:10.1242/jcs.196642

We report here that BCAP is also a centriolar satellite protein. We detect two isoforms in our cell lines. Both inhibit ciliogenesis but appear to have subtly different roles in this process.

RESULTS

BCAP (ODF2L/ODF2-like) is a centriolar satellite protein

We previously have investigated the role of centrosome proteins in neural progenitor divisions in the zebrafish retina (Novorol et al., 2013). One protein we depleted from zebrafish embryos was ODF2, a component of the appendages of the mother centriole (Lange and Gull, 1995). Depleting this protein was not embryonic lethal but did result in various defects, including smaller eyes and brain. Since the sequence databases of mammalian species contain a sequence annotated as a related protein, ODF2-like or ODF2L, we sought to characterise this protein to see if it could be acting redundantly with ODF2. It has previously been named as BCAP (basal body, centriole-associated protein), and was described to be localised to the basal bodies of multi-ciliated tracheal cells (Ponsard et al., 2007).

We first tested the localisation of BCAP within human cell lines by using the few commercially available antibodies and found one – Biorbyt orb31049, hereafter referred to as anti-BCAP (Biorbyt) antibody – that gave staining near the centrosome. We expected to see BCAP localisation at one of the two centrioles only, because the centriolar appendages – of which ODF2 is part – are present on the mother but not daughter centriole (Lange and Gull, 1995; Mogensen et al., 2000; Nakagawa et al., 2001). Instead, we observed a speckled staining of numerous small punctae forming a cloud around the centrioles of the centrosome, visualised by staining for γ-tubulin (Fig. 1A-C,I).

To confirm the specificity of the stining of the anti-BCAP (Biorbyt) antibody we decided to test if it would bind to GFP-BCAP expressed in cells. HeLa cells were transfected with a plasmid encoding GFP-BCAP and then stained with anti-γ-tubulin or anti-BCAP (Biorbyt) antibody. GFP-BCAP was strongly stained by the anti-BCAP (Biorbyt) antibody (Fig. 1D-F), its staining overlapping with green fluorescence from GFP-tagged BCAP (GFP-BCAP). The green fluorescence from GFP-BCAP was punctate in nature and present as a cloud around the centrosome (Fig. 1G).

This staining pattern is characteristic of centriolar satellites (Tollenaere et al., 2015), protein-dense structures that are involved in transport to and from the centrosome. The prototypical centriolar satellite protein is PCM-1 (Balczon et al., 1994; Kubo et al., 1999), whose staining (Fig. 1H) resembles that of BCAP. We, therefore, tested if the localisation of BCAP coincided with that of PCM-1 by staining human cell lines transfected with GFP-BCAP with anti-PCM-1 antibody. There was nearly complete overlap between the signals (Fig. 1J-L). This is consistent with BCAP being a centriolar satellite protein.

The structure of satellites and the localisation of many other proteins to these structures depends on the presence of PCM-1 (Stowe et al., 2012). When we depleted PCM-1 using RNA interference (RNAi), the localisation of the BCAP signal changed. There was no centriolar satellite staining but, instead, a diffuse and non-punctate cytoplasmic staining was observed (Fig. 1M-O). This is again consistent with BCAP being a centriolar satellite protein.

Since some proteins have multiple locations within the cell or within a particular organelle, such as OFD1 being located at the centriolar appendages and in the centriolar satellites (Ferrante et al., 2009; Singla et al., 2010; Tang et al., 2013), we carefully examined the localisation of BCAP in multiple cells. In many cells, we could observe BCAP staining around but not overlapping with that of γ-tubulin that stains the material immediately around the centrioles (Fig. 1I).

Since BCAP has a different localisation from ODF2, we re-examined the homology between BCAP and ODF2. The two proteins only share 51% amino-acid sequence similarity and 28% identity, in a region comprising less than half of the protein length. We then explored the relationship between ODF2 and BCAP by constructing a phylogentic tree (Fig. 2A). We compared BCAP and ODF2 sequences from different animals, representing amphibians (*Xenopus tropicalis*), reptiles (*Anolis carolinensis*), birds (chicken, *Gallus gallus*) and rodents (domestic mouse, *Mus musculus*), with the human sequences. All BCAP sequences grouped together, separate from the group of ODF2 sequences. There is a clear split between BCAP and ODF2, implying they diverged at the latest in the last common ancestor for crown group tetrapods. ODF2L/ODF2-like is, therefore, a potentially misleading name for BCAP. We will continue to use the name BCAP, as first proposed by Ponsard et al. to refer to this protein from now on. The relationship between the different isoforms of BCAP, those described by Ponsard et al. and those predicted in the NCBI database, is shown in Fig. 2B, together with the binding sites of the antibodies and small interfering RNAs (siRNAs) used in this study.

The role of BCAP in ciliogenesis

Centriolar satellites are important for ciliogenesis and the localisation of component proteins changes during this process (Kubo et al., 1999; Stowe et al., 2012). We, therefore, tested the localisation of BCAP using RPE1-hTERT cells that had been induced to ciliate by serum starvation (Fig. 3). The anti-BCAP (Biorbyt) antibody showed clear satellite staining in RPE1-hTERT cells under serum-supplemented, proliferating conditions (Fig. 3A) but did not stain the region around the centrioles/basal bodies in serum-starved RPE1-hTERT cells, implying that BCAP had disappeared during ciliogenesis (Fig. 3B). Whether this was by degradation or dispersal could not be determined by immunofluorescence alone. Overexpression of GFP-BCAP gave a surprising result. Staining was observed around the centrioles/basal bodies with the expected pattern but we did not observe any transfected cells with cilia in serum free-medium, as visualised by staining of acetylated tubulin (Fig. 3C,D,E). This suggested that BCAP can act to suppress the formation of cilia.

We assayed how expression levels of BCAP differed before and after ciliation. Western blotting of extracts of RPE1-hTERT and HeLa cells with the anti-BCAP (Biorbyt) antibody under serum-supplemented (non-ciliating) and serum-free (ciliating) conditions showed that BCAP was readily detectable in serum-supplemented conditions but absent when cells had ciliated (Fig. 3F,G). This suggests that during ciliogenesis existing BCAP is not dispersed from the centriolar satellites but removed from the cell.

If BCAP normally acts as a ciliogenesis inhibitor, then depletion of BCAP might allow for cilia to be made under conditions in which cells normally maintain a centrosome. We depleted all isoforms of BCAP by RNAi (two separate siRNAs, locations of target sites shown in Fig. 2B). Depletion was confirmed by reverse transcriptase (RT)-PCR (Fig. 4A,B) and immunocytochemistry (Fig. 4C). When RPE1-hTERT cells were transfected with BCAP siRNAs in serum-supplemented medium, i.e. conditions under which they normally do not ciliate, cilia were now extensively generated (Fig. 4E,F). Cilium length was also increased by a quarter, from 3.1 to 4.1 µm ($P<0.001$ by ANOVA, both siRNAs) (Fig. 4G-I). This knockdown could be rescued by overexpressing mouse BCAP, whose coding sequence is not completely identical with human

Journal of Cell Science (2017) 130, 3360-3373 doi:10.1242/jcs.196642

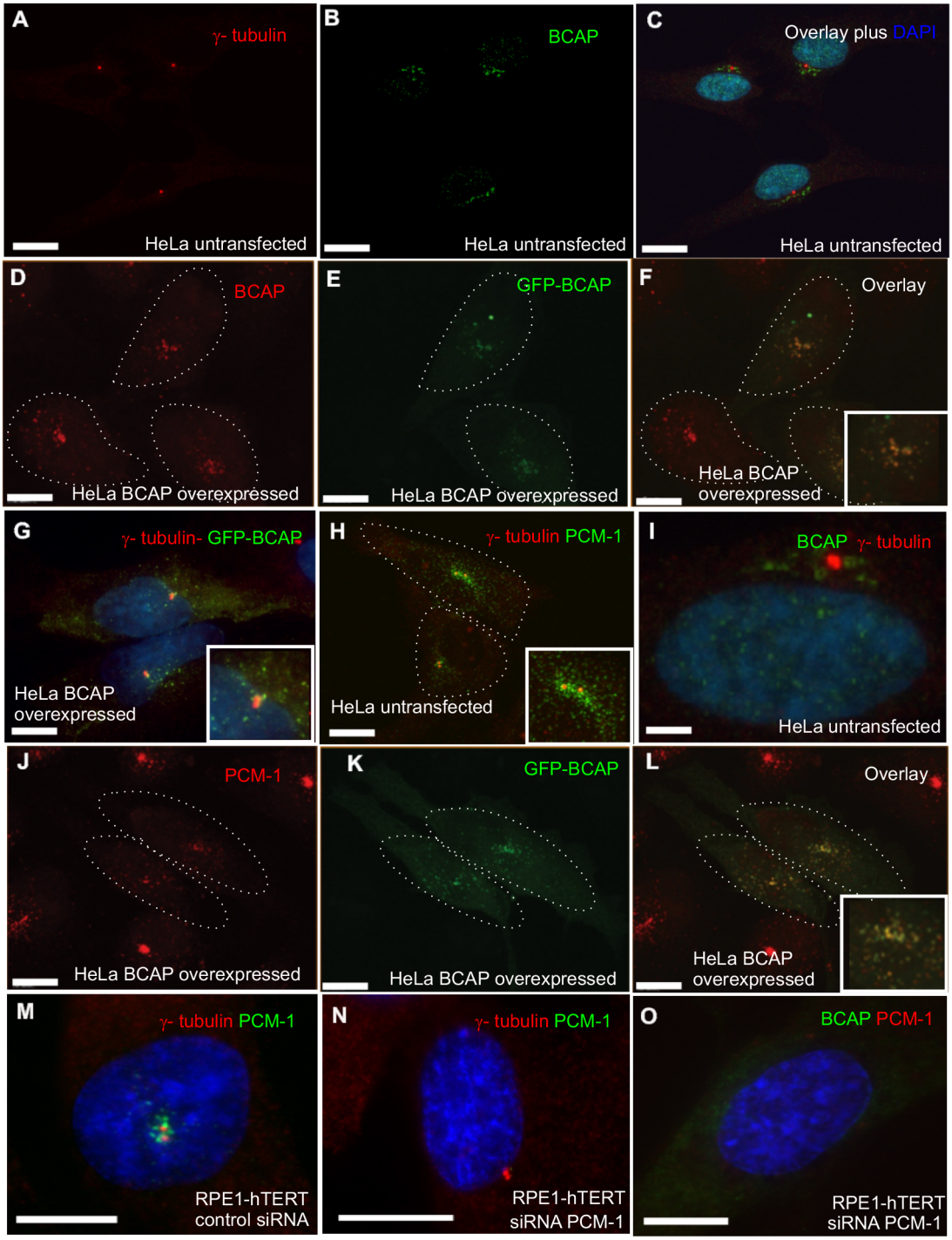

Fig. 1. Localisation of ODF2-like/BCAP. (A-C) HeLa cells stained with anti-γ-tubulin antibody (A, red), anti-BCAP (Biorbyt) antibody (B, green) and DAPI (blue in combined image, C) showing a cloud of small spots clustered around the centrosome, 1–2 punctae of γ-tubulin. (D-F) anti-BCAP staining (red, D) coincides with GFP-BCAP fluorescence (green, E), the overlaid signals are shown in F. (G) GFP-BCAP (green) displays a punctate staining around the centrosome, cells stained with anti-γ-tubulin antibody (red), DAPI in blue. (H) HeLa cells stained with anti-PCM1 antibody (green) show a similar pattern of staining, characteristic of centriolar satellites. (I) For BCAP (green), staining is around the centrosome but not on the centrioles: γ-tubulin (red) staining does not overlap with BCAP. This is a magnified part of the image shown in C. (J-L) PCM-1 staining (red, J) coincides with GFP-BCAP staining (green, K), the overlaid signals shown in (L). (M) PCM1(green), γ-tubulin (red) are unaffected in control siRNA cells. (N) PCM-1 (green) is depleted by RNAi using an siRNA targeting PCM-1 (γ-tubulin in red). (O) siRNA depletion of PCM-1 results in BCAP (green) no longer localising at the satellites. Instead, a diffuse, non-punctate cytoplasmic staining is observed. Scale bars: 10 µm (A-D, F-O), 2 µm (E).

BCAP at the target sites of the two siRNAs used. When cells were depleted of BCAP by transfection of siRNA while simultaneously transfected with an expression construct for mouse BCAP, no cilia were formed (Fig. 4K-N). Together, these overexpression and/or depletion experiments are consistent with BCAP acting as a ciliogenesis inhibitor.

Journal of Cell Science (2017) 130, 3360-3373 doi:10.1242/jcs.196642

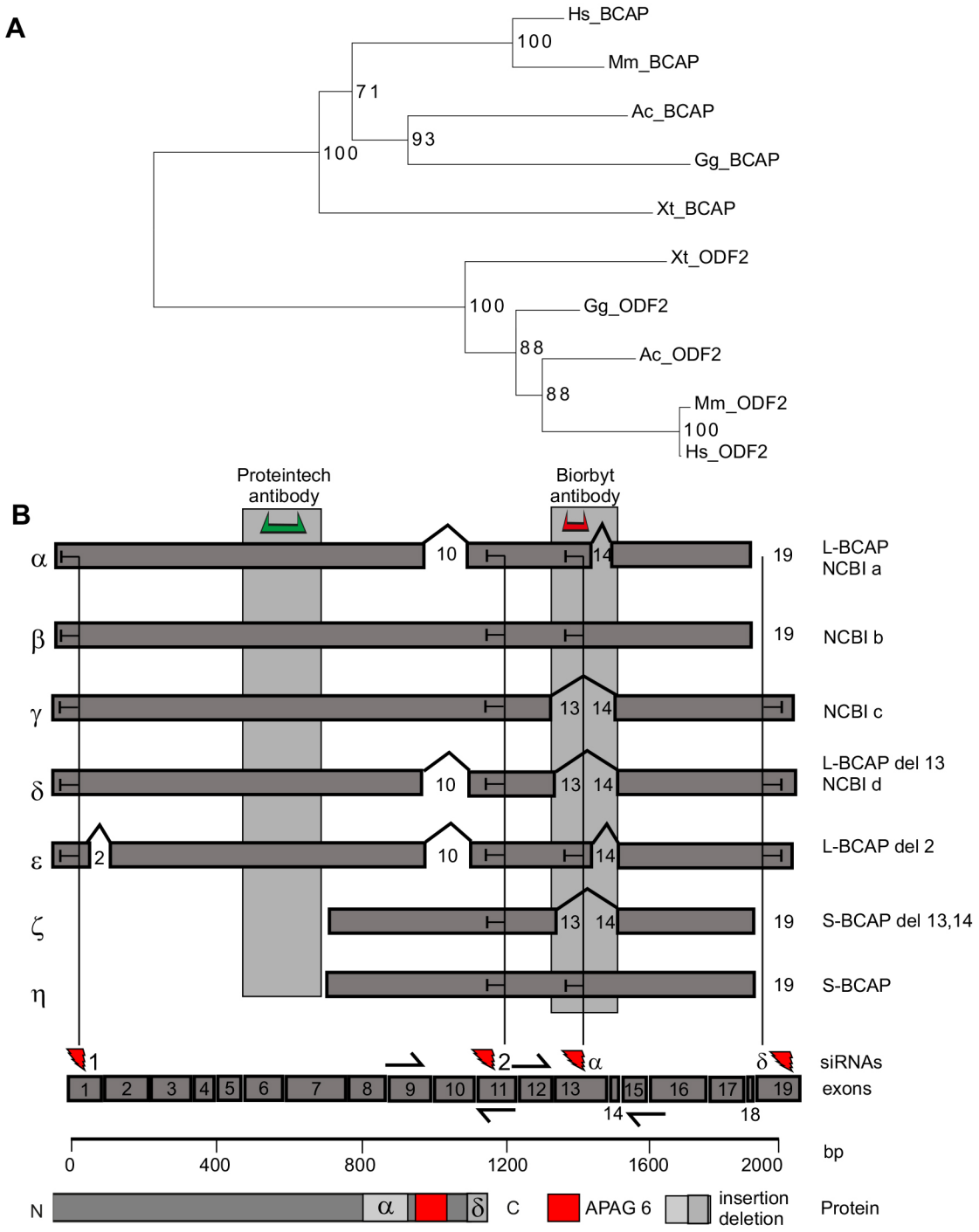

Fig. 2. Phylogenetic analysis and gene structure of BCAP. (A) Phylogenetic analysis of the relationship between BCAP and ODF2. Sequences used were from *Xenopus tropicalis* (Xt), *Anolis carolinensis* (Ac), *Gallus gallus* (Gg), *Mus musculus* (Mm) and *Homo sapiens* (Hs). The tree was constructed using CLC Genomics. Bootstrap support values are indicated above branches. (B) Schematic of the BCAP gene and BCAP isoforms. The NCBI database and Ponsard et al. (2007) have predicted/observed several transcripts and isoforms. These are summarised here. We have named them α–η in order to avoid confusion. NCBI numbering (a-d) and Ponsard et al. (2007) naming schemes (S/L-BCAP del x) are also shown for completeness. In isoforms where exons are skipped, the number of the skipped exon is in the gap between the two exons that are incorporated. Single-headed arrows show the binding sites for primers used to determine which variants are present. Target sites for the siRNAs used in this study are shown in red at the base of the diagram, lines with blunt arrowheads show which isoforms are be targeted. The α and δ protein isoforms differ in the C-terminus, with BCAPα having a 50 amino acid insertion by inclusion of exon 13 compared to BCAPδ, which possesses an additional 20 amino acids in the tail due to inclusion of exon 19 instead of exon 18. The anti-BCAP (Biorbyt) antibody was raised against the C-terminus of BCAPα, whereas the anti-BCAP (Proteintech) antibody binds the N-terminus of BCAP and, so, will detect both BCAPα and BCAPδ. The APAG6 domain is coloured red in the schematic, with the inserted/deleted sequences of the α/β isoforms shown as grey shades.

Depletion of BCAP did not alter the pattern of staining of ODF2, γ-tubulin or PCM-1 (Fig. 4O-Q). Centriolar satellite and centrosome structure would, therefore, appear not to be grossly affected by BCAP depletion, as these markers for the satellites, pericentriolar matrix and appendages showed normal localisation when BCAP was absent.

Journal of Cell Science (2017) 130, 3360-3373 doi:10.1242/jcs.196642

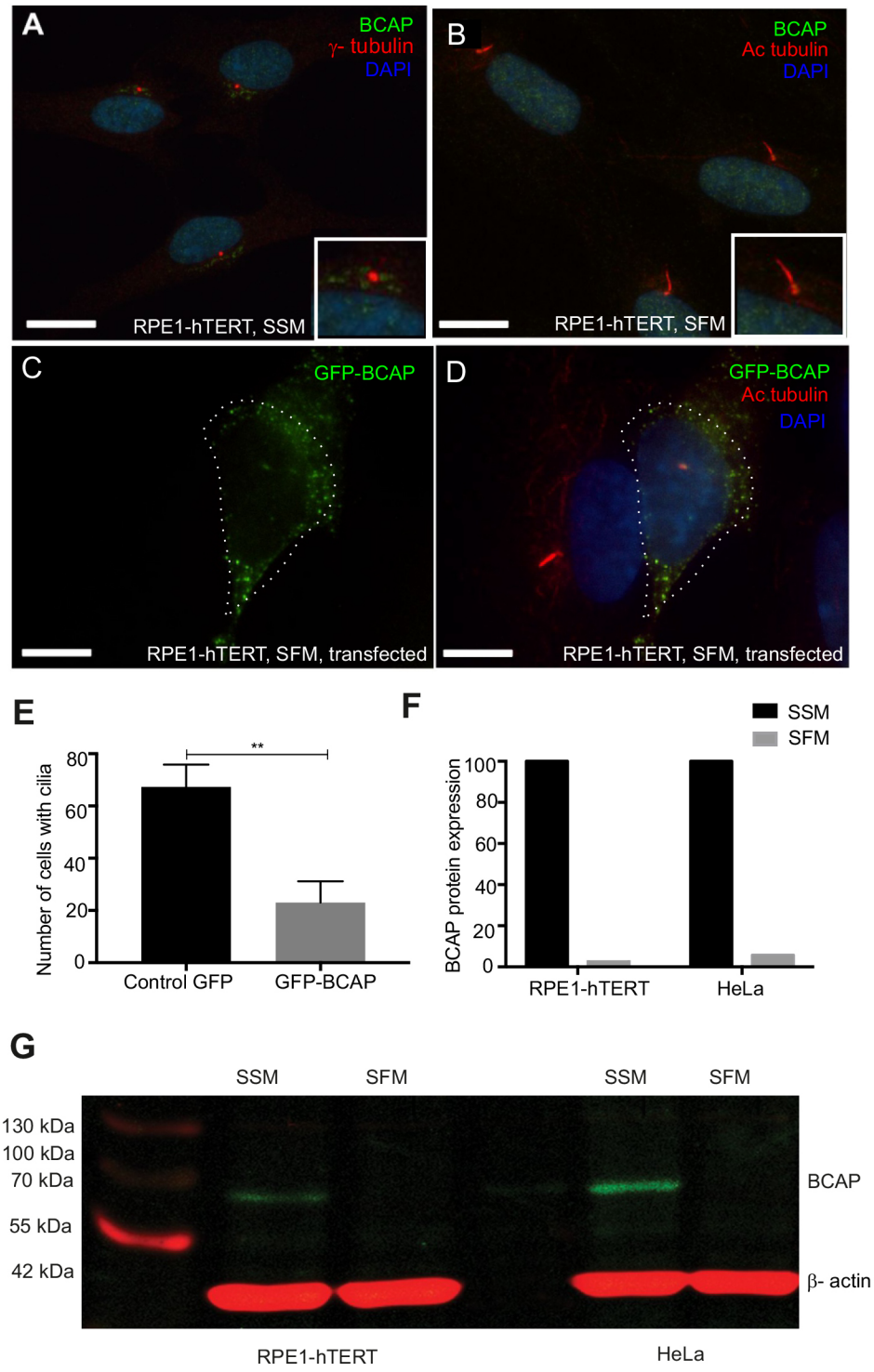

Fig. 3. BCAP and ciliogenesis. (A) In proliferating RPE1-hTERT cells in serum-supplemented medium (SSM), endogenous BCAP (anti-BCAP (Biorbyt) antibody, green) localises in satellites around the centrosome (γ-tubulin, red) next to the nucleus (DAPI, blue). (B) In serum-free medium (SFM), cilia (acetylated tubulin, red) are formed and BCAP staining (green) disappears (DAPI in blue). (C,D) When cells are transfected with a GFP-BCAP expression plasmid [C, GFP only; D, GFP plus acetylated tubulin (red) and DAPI (blue)], untransfected cells (left-hand cell) form a cilium, whereas transfected cells do not (right-hand cell). (E) There is a 40% reduction in the number of cells with cilia when GFP-BCAP is expressed (P<0.001 by Student's t-test, 100 cells counted, n=3). (G) Western blotting confirms that BCAP (green; running at ~70 kDa), does not disperse, instead the protein disappears. This is quantified in F. Scale bars: 10 µm.

BCAP has multiple isoforms, two of which are present in RPE-hTERT cells

When we repeated these experiments with a different anti-BCAP antibody, i.e. 23887-1-AP from Proteintech [anti-BCAP (Proteintech) antibody], we obtained slightly different results. Proliferating cells still showed a satellite pattern of staining (Fig. 5A-C) but, as shown by western blotting, BCAP remained present after ciliogenesis had completed, although at reduced levels (30% reduction, Fig. 5D,E). By immunofluorescence, in a mixed population of RPE1-hTERT cells at different stages of ciliogenesis, a proportion of cells showed no staining and another showed satellite staining around the basal bodies (Fig. 5F-H). This staining overlapped with that of PCM-1 (Fig. 5I) and partially with that of γ-tubulin (Fig. 5J), in that centrioles as well as satellites were stained. Notably, the staining pattern was not restricted to one centriole like for ODF2 (Fig. 5K).

We sought to image how BCAP localisation, as visualised by the anti-BCAP (Proteintech) antibody, changes during ciliogenesis. We synchronised cells with a nocodazole block, then released them into medium lacking serum and fixed samples every hour. These

Journal of Cell Science (2017) 130, 3360-3373 doi:10.1242/jcs.196642

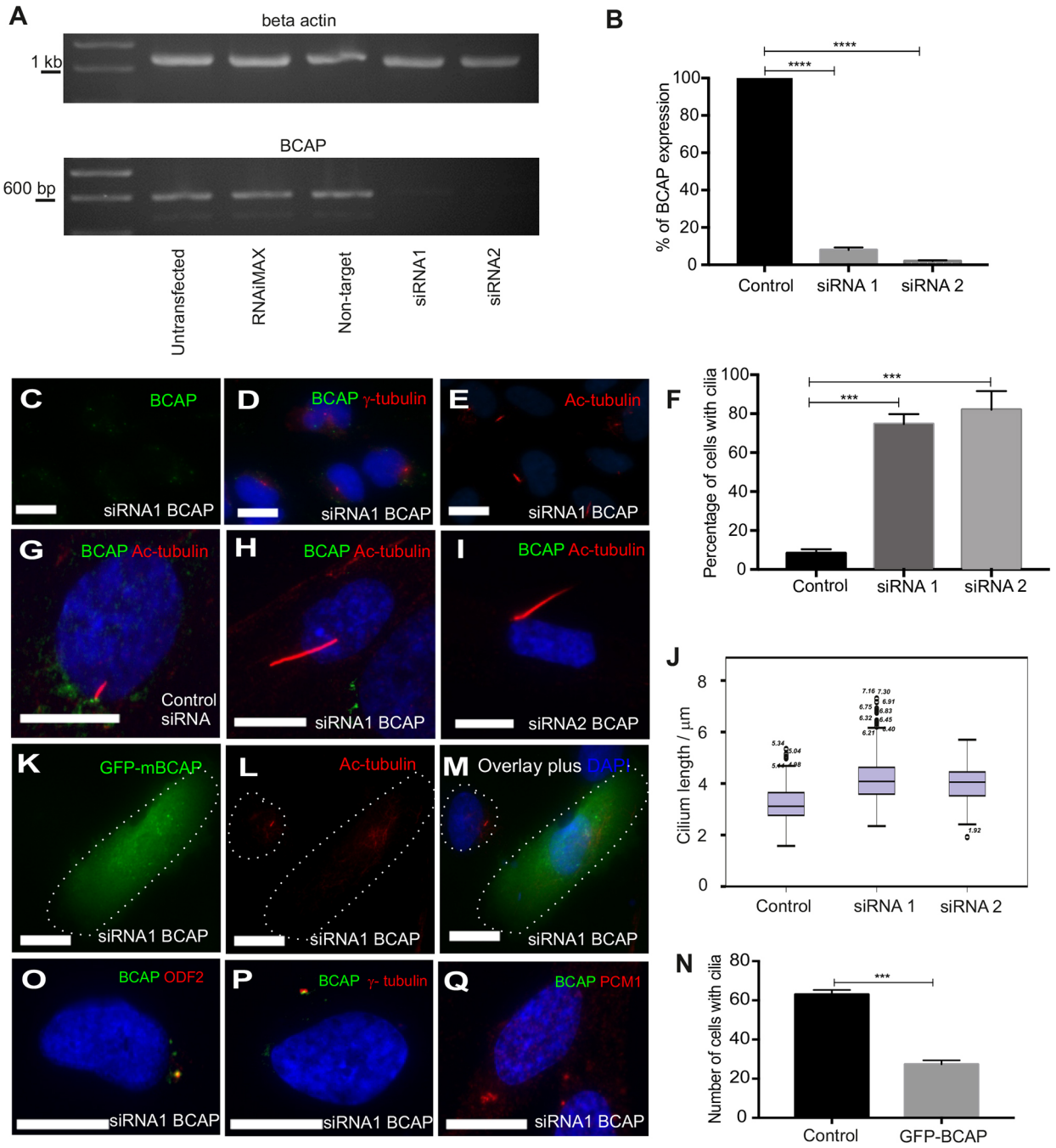

Fig. 4. BCAP depletion promotes ciliogenesis. (A,B) Two different siRNA duplexes both effectively deplete BCAP: a 600 bp fragment of *BCAP* is amplified by RT-PCR in various control samples (untransfected, lipofectamine and non-target siRNA) but is absent when proliferating RPE1-hTERT cells are treated with the siRNAs; beta actin is amplified to the same level in all samples (three independent experiments $P<0.001$ by one-way ANOVA). (C) By immunofluorescence, BCAP signal disappears in siRNA-treated cells (BCAP signal alone in green). (D) γ-tubulin signal is unaffected by BCAP depletion (γ-tubulin in red, BCAP in green, plus DAPI in blue). (E) A large proportion of these cells in serum-supplemented medium now form cilia (acetylated tubulin in red). (F) Only 7% of control cells form cilia but 79% of cells treated with siRNAs ciliate; a total of 100 cells were counted, $P<0.001$ by chi-squared. These data are from one experiment; three repeats show similar results. (G-I) Cilium length also increases in serum-starved and BCAP-depleted RPE1-hTERT cells from 3–4 µm, $P<0.001$ by Student's *t*-test, 150 cilia were counted in each sample. (J). Examples of control cilia are shown in G, long cilia observed after siRNA treatement shown in H and I. (K-N) Mouse BCAP will rescue RNAi-depletion, with transfected cells not making cilia, shown separately in L and with DAPI and GFP-BCAP together in M (N, $P<0.001$; Student's *t*-test, 100 cells were counted in three separate repeats). BCAP staining is much reduced in BCAP siRNA-treated cells (O-Q). However, γ-tubulin (P) and PCM-1 (Q) staining are unaffected. Scale bars: 10 µm.

samples were then stained with the anti-BCAP (Proteintech) antibody (Fig. 6A) and anti-acetylated tubulin antibody.

BCAP staining changed during the course of ciliogenesis. Immediately after release from the nocodoazole block, BCAP staining presented as a scattered pattern (Fig. 6A). BCAP then adopted a more satellite-like appearance within an hour. As ciliogenesis started, all BCAP staining disappeared, with only negligible fluorescence signal remaining (Fig. 6B). As ciliogenesis

Journal of Cell Science (2017) 130, 3360-3373 doi:10.1242/jcs.196642

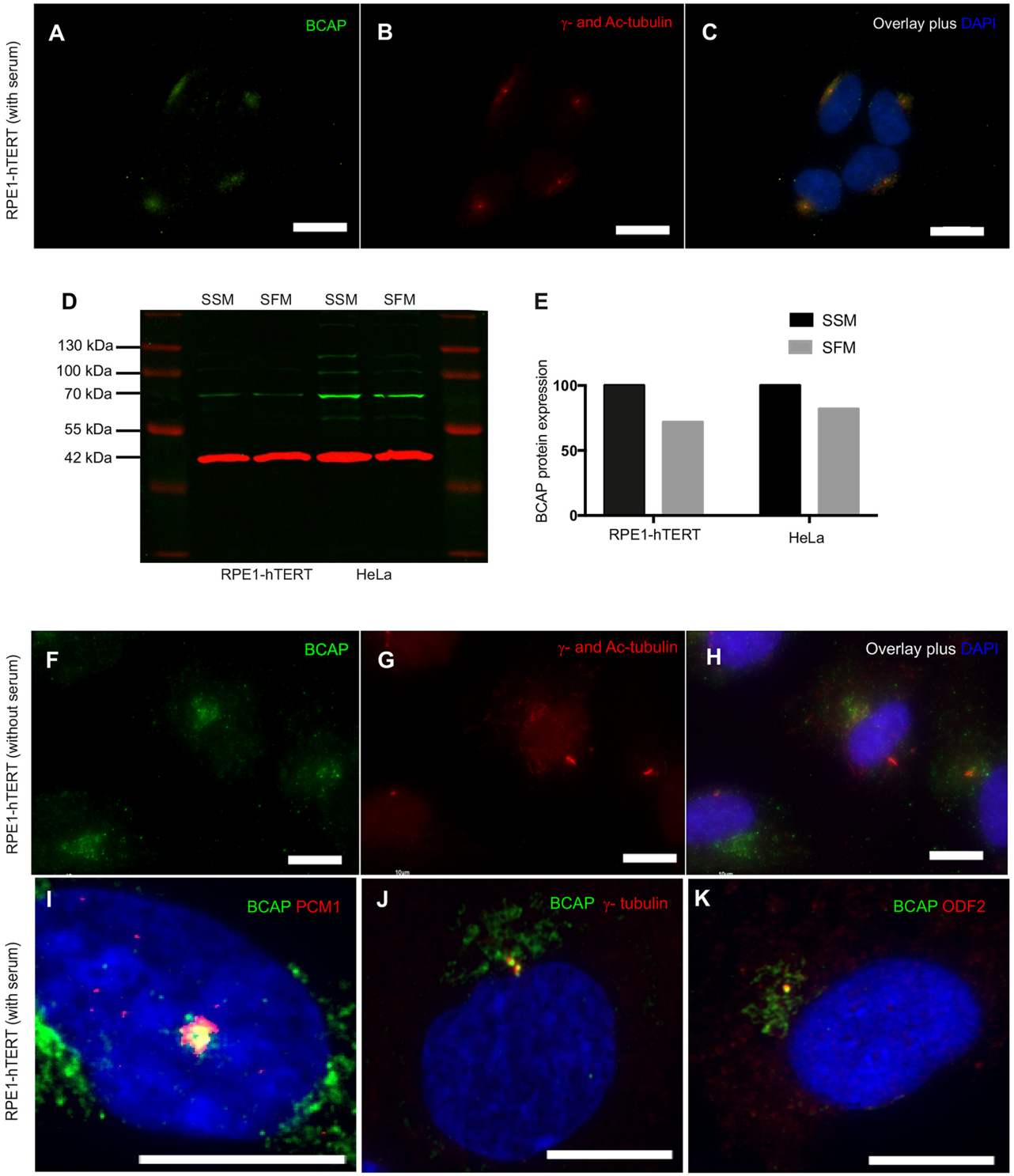

Fig. 5. BCAP consists of at least two isoforms. (A-C) In proliferating RPE1-hTERT cells in serum-supplemented medium (SSM), the anti-BCAP (Proteintech) antibody (green) shows satellite staining around the centrosomes (γ-tubulin, red). (D,E) In contrast to the western blot using the Biorbyt antibody as probe, when the anti-BCAP (Proteintech) antibody (green) was used to probe cell extracts before and after ciliogenesis, levels of this protein decrease slightly rather than disappear, quantified in E. β-actin is stained in red. (F-H) In serum-free medium (SFM), cells at presumably different stages of ciliogenesis can be observed. BCAP can be observed at the base of the cilium or clustered away from it. (I) The anti-BCAP (Proteintech) antibody staining (green) colocalises with that of PCM-1 (red). (J) Satellite-like staining of BCAP from the anti-BCAP (Proteintech) antibody (green) but with some overlap with the γ-tubulin signal (red). (K) As expected, ODF2 (red) shows a single punctum of signal (the mother centriole) in contrast to the staining from the anti-BCAP (Proteintech) antibody (green). Scale bars: 10 µm.

neared completion at 8 h (Fig. 6C), BCAP staining was again observed in the centriolar satellites (Fig. 6A), with BCAP returning to 50% of pre-ciliogenesis level (Fig. 6B).

The different results from the two anti-BCAP antibodies could be explained by the existence of multiple isoforms of BCAP. ENSEMBL and NCBI databases predict several splice variants of

Journal of Cell Science (2017) 130, 3360-3373 doi:10.1242/jcs.196642

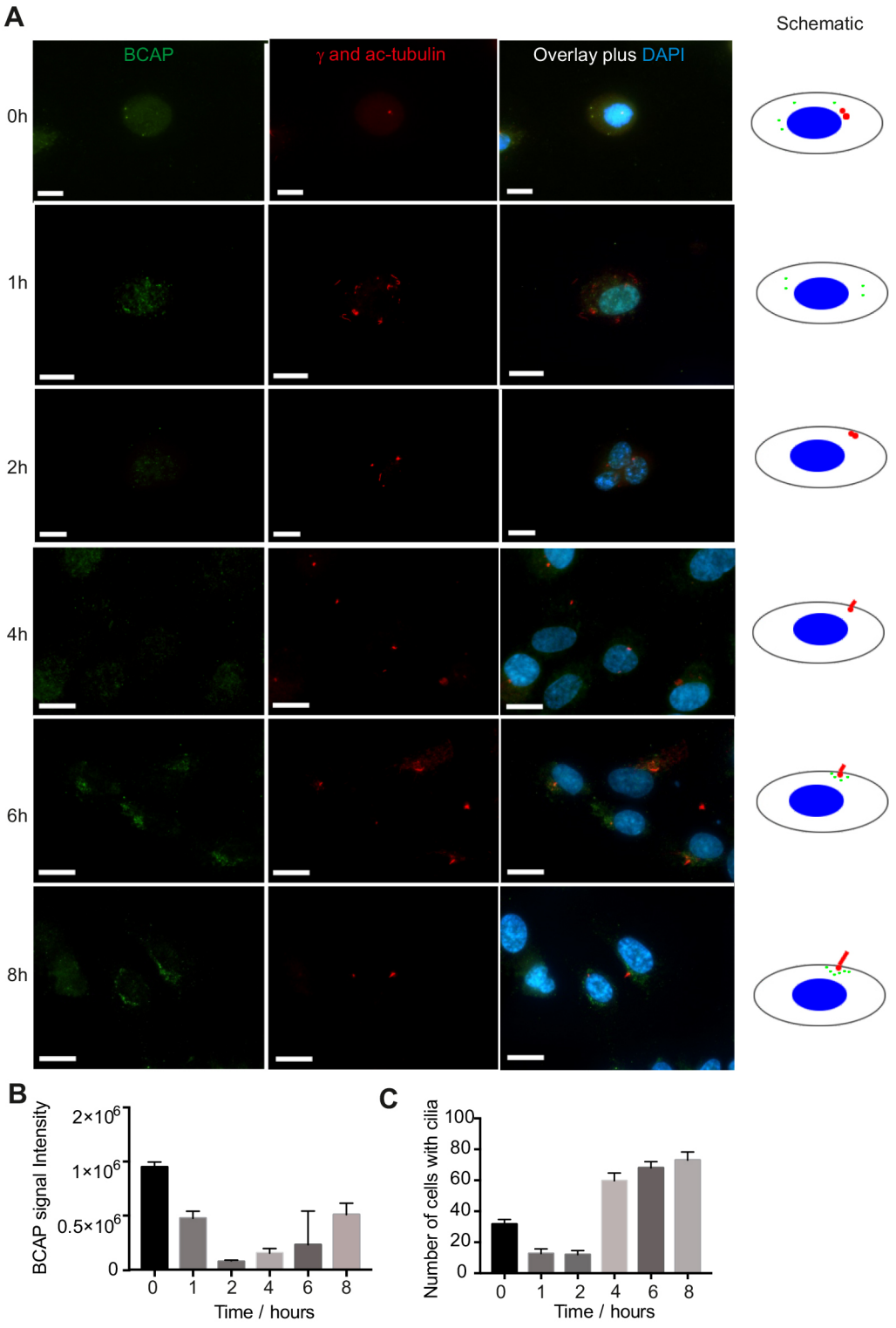

Fig. 6. BCAP levels and localisation change during ciliogenesis. RPE1-hTERT cells were synchronised by a nocodazole block followed by release. Samples were fixed at hourly intervals, with timepoints at which key changes took place shown here. After release at 1 h, BCAP (green) is dispersed in the cytoplasm, as is the γ-tubulin signal (red). While the γ-tubulin signal reorganises into recognisable centrosomes between 2–4 h, BCAP signal disappears. At 6 h, cilia are visible and BCAP signal is returning. By 8 h, ciliogenesis appears complete and strong BCAP signal is visible at the base of cilia. Cells were also stained with DAPI (blue). The right hand column summarises these changes, with satellites/BCAP as small green dots, the centrioles/basal body/cilium in red and nucleus in blue. (B) Signal intensity of BCAP was measured at each stage. BCAP is highly expressed at the first time-point and then gradually decreases. By 8 h its expression has increased again to 50% of its pre-ciliation value. (C) Number of cilia at each time point was measured, with 60% of cells showing cilia by 8 h. This represents three independent experiments. Scale bars: 10 µm.

BCAP based on genomic and EST data (Fig. 2B), and Ponsard et al. (2007) describe five isoforms. We have combined these data in Fig. 2B, using Greek letters to label the combined set, but also showing the names used by Ponsard et al. and the NCBI database, on the right-hand side of the figure. There are five long isoforms, all of similar size, which vary by the inclusion of exons 2, 10, 13 and 14, plus two short isoforms that include exon 10 but differ by the presence/absence of exons 13 and 14.

We tested RPE-hTERT cells for the presence of these isoforms using RT-PCR. With the primer pair to test for inclusion/skipping of exon 10, we observed only the smaller band that was produced if exon 10 was skipped (Fig. 7A). This is consistent with the short isoforms and two of the long isoforms being absent, i.e. isoforms β, γ, ζ and η. For exon 13, we observed both larger and smaller bands that would be produced if this exon were either included or skipped in different isoforms. These data are consistent with the presence of

Journal of Cell Science (2017) 130, 3360-3373 doi:10.1242/jcs.196642

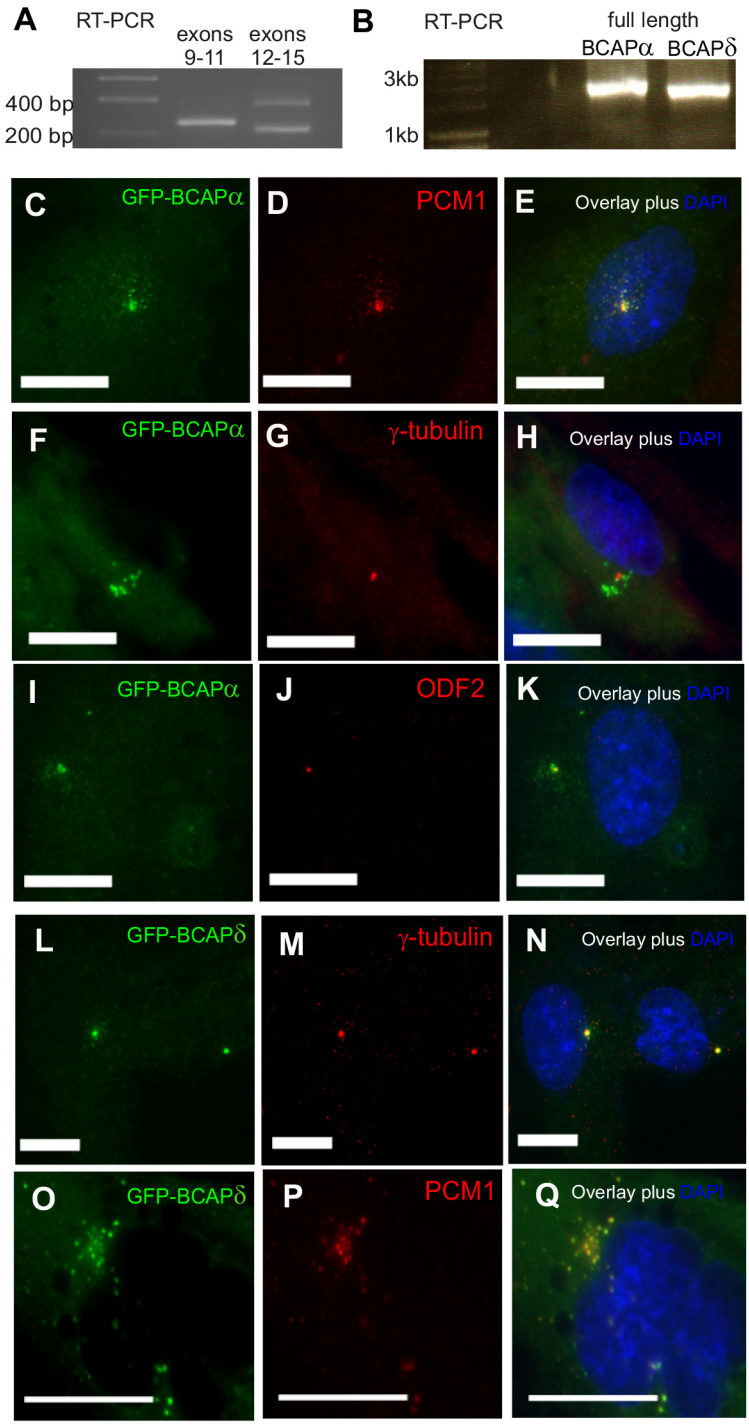

Fig. 7. BCAP exists as multiple isofroms, two are present in RPE1-hTERT cells. (A) RT-PCR using primers to amplify exons 9–11 yields one smaller band corresponding to skipping of exon 10. RT-PCR with primers to amplify exons 12–15 yields two bands corresponding to inclusion or skipping of exon 13. (B) Full-length BCAPα and δ are present in RPE1-hTERT cells. There is only one band for BCAPδ but the primers would also amplify the shorter BCAPε if it were present. (C-E) GFP-BCAPα shows a satellite-like staining that colocalises with that of PCM-1 (red). (F-H) This GFP-BCAPα signal is around but not overlapping γ-tubulin (red). (I-K) GFP-BCAPα forms a cloud of punctae around the single ODF2 punctum (red). (L-N) GFP-BCAPδ shows a pericentriolar/centriolar-like staining, overlapping γ-tubulin in about 80% of cells. (O-Q) GFP-BCAPδ shows a satellite-like staining overlapping PCM-1 (red) in about 20% of cells. Scale bars: 10 µm.

the α, δ and ε isoforms (Fig. 2B). When we cloned and sequenced BCAPδ and BCAPε, we observed only the δ isoform (Fig. 7B) and, similarly, we observed only one band when amplifying BCAPα. In our cells, it would appear that only the α and δ isoforms are present. Compared to BCAPα, in BCAPδ exon 13 is skipped but exon 19 substitutes for the very short exon 18 that is incorporated in BCAPα. BCAPα and δ will, therefore, have almost identical molecular masses of 69 kDa.

The anti-BCAP (Biorbyt) antibody was raised to recognise the C-terminus of BCAPα, whereas the anti-BCAP (Proteintech) antibody was raised to recognise the common N-terminus of both α and δ isoforms (Fig. 2B). The results above suggest that, in RPE-hTERT, cells two isoforms of BCAP exist with slightly different expression patterns. BCAPα is completely removed in ciliated cells. BCAPδ returns to cells that have made cilia.

To further refine the roles of the two variants, we cloned the human BCAPα and BCAPδ. GFP-BCAPα showed centriolar satellite staining and no centriolar staining (Fig. 7C-K), consistent with the antibody staining. In contrast, GFP-BCAPδ showed centriolar and satellite staining (Fig. 7L-Q). The antibody against all isoforms (α to η) of BCAP, raised by Ponsard et al. (2007), stained centrosomes, centrioles and basal bodies in human nasal epithelial (HNE) cells.

We depleted each isoform separately. By using RT-PCR, depletion was 89% and 80%, respectively, for BCAPα and BCAPδ (Fig. 8A,

Journal of Cell Science (2017) 130, 3360-3373 doi:10.1242/jcs.196642

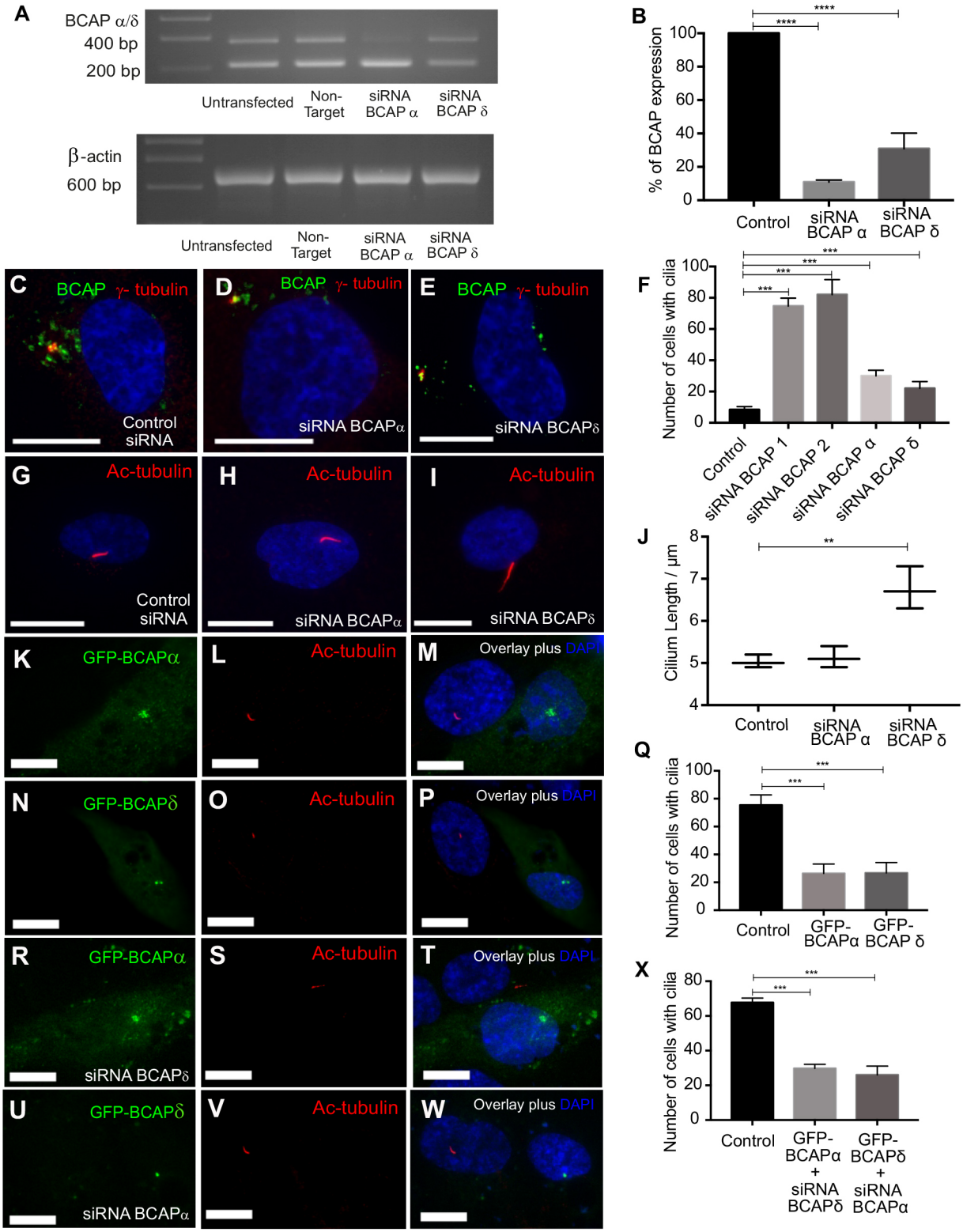

Fig. 8. BCAPα and δ have overlapping but subtly distinct roles in ciliogenesis. (A-B) BCAPα and BCAPδ were depleted individually by siRNA. The amount of depletion of each isoform was assessed quantitatively by RT-PCR (P<0.001; one-way ANOVA, three repeats). (C-E) Depletion of either BCAPα or δ individually reduces but does not eliminate staining by the Proteintech antibody (green), which binds both isoforms. γ-tubulin staining (red) shows the centrioles and pericentriolar matrix are mainly intact. (F) Depletion of either isoform, BCAPα or δ, individually causes cells to form cilia in serum supplemented conditions (P<0.001; one-way ANOVA, 100 cells counted in three repeats). (G-I) In BCAPδ- but not BCAPα-depleted cells longer cilia are observed, quantified in J (P<0.001 by one-way ANOVA, 100 cells counted in three repeats). (K-P) Expressing either GFP-BCAPα or δ in serum-free conditions suppresses normal ciliation. Left-hand cell is untransfected, right hand cell is transfected. Cilia labelled with anti-acetylated tubulin (red). This is quantified in (Q) (P<0.001 by one-way ANOVA, 100 cells counted in three repeats). (R-X) GFP-BCAPα can rescue BCAPδ-siRNA, with cells not making cilia in serum-supplemented conditions (cilia/acetylated tubulin in red). The same is true for the reciprocal experiment. This is quantified in (X) (P<0.001 by one-way ANOVA, 100 cells were counted in three repeats). Scale bars: 10 µm.

Journal of Cell Science (2017) 130, 3360-3373 doi:10.1242/jcs.196642

B). In both cases, the anti-BCAP (Proteintech) antibody staining decreased but was not eliminated, consistent with it binding both isoforms (Fig. 8C-E). Depletion of either protein by using a variant-specific siRNA resulted in ciliogenesis under serum-supplemented conditions. 30% of cells now formed cilia when either BCAPα or BCAPδ was depleted alone, compared to 70% when both isoforms were depleted together (Fig. 8F). This is consistent with the two isoforms acting together to suppress ciliation.

When either BCAPα or BCAPδ was depleted from cells undergoing serum starvation, cilia formed as expected but it was notable that cilium length increased in BCAPδ-depleted cells but not in those depleted of BCAPα (Fig. 8G-J).

Overexpression of either GFP-BCAPα or GFP-BCAPδ suppressed cilium formation in serum-free medium, consistent with our previous observations (Fig. 8K-P). The proportion of cells with cilia decreased from 80% to 25% in both cases (Fig. 8Q). There appears to be partial redundancy regarding the roles of BCAPα and BCAPδ, since overexpressing BCAPα in cells depleted of BCAPδ suppresses ciliation and the reciprocal experiment yields the same result (Fig. 8R-X).

These data suggest that BCAP exists as two isoforms in RPE1-hTERT cells. Both isoforms are removed during ciliogenesis but one, BCAPδ, reappears once ciliogenesis has completed. Both suppress ciliation but, additionally, BCAPδ acts to control cilium length once cilia have formed.

BCAP depletion does not affect microtubule regrowth and reorganisation or the cell cycle

Since other ciliogenesis inhibitors, such as OFD1 and CP110, have additional centrosome/centiole-based functions (Schmidt et al., 2009; Singla et al., 2010), we assayed BCAP for other roles at the centrosome. We first tested if BCAP has a role in microtubule nucleation, a major function of the centrosome in interphase cells (Bornens, 2002; Tassin and Bornens, 1999), by using the microtubule regrowth assay (Fry et al., 1998). BCAP-depleted cells (both isoforms; siRNA1) showed no detectable difference in the time at which microtubule nucleation restarted or the rate at which the network was re-established, compared to control-treated cells (Fig. S1A-J). BCAPα and δ are, therefore, not required for microtubule nucleation. At the zero time point, the microtubule network in BCAP-depleted cells appeared to be similar to that of control cells, so the mature microtubule network seems unaffected by removal of BCAPα/δ.

We also tested whether BCAP is required for adjusting an existing microtubule network. We used the wound assay on confluent RPE1-hTERT cells to test if BCAP (either isoform) has a role in cell migration and polarity through the centrosome (Nobes and Hall, 1999; Luxton and Gundersen, 2011). In both control and siRNA-transfected cells, the wound closed at the same rate (Fig. S1K-P). Staining the cells for Golgin-97 and γ-tubulin showed that both BCAP-depleted and control cells behaved the same, with the Golgi complex and centrosome reorientating towards the direction of the wound during closure (Fig. S1Q,R). By this assay, depletion of BCAP (both isoforms) neither inhibits migration nor adversely affects cell polarity.

Finally, we tested for a role of BCAP in the cell cycle. The centrosome contributes to the poles of the mitotic spindle and has a critical role both in nucleating astral microtubules and facilitating the fast generation of a mitotic spindle (Basto et al., 2006; Stevens et al., 2007). Furthermore, depletion of many centrosome proteins results in a G1 arrest before the cells commit to entering the cell cycle (Mikule et al., 2007). We found that, after 24 h in culture, BCAP-depleted RPE1-hTERT cells showed the same distribution of cell cycle phases as control treated cells (Fig. S2A,B), including after first serum-starving the cells for 24 h (Fig. S2C,D). Thus BCAP depletion (both isoforms) does not cause a G1 block nor does it prevent progression into mitosis. On balance, the role of BCAP appears to be specific to the regulation of ciliogenesis.

DISCUSSION

We here describe BCAP as a centriolar satellite protein that acts as an inhibitor of ciliation, specifically, the initiation of ciliogenesis. Overexpression of BCAP in cells, under conditions that normally cause cells to form cilia, prevents this from occurring. Depletion of BCAP under conditions in which ciliation is not normally observed results in a substantial proportion of cells producing cilia.

Many centrosome proteins, including those in the satellites, have been shown to contribute to ciliogenesis. Few proteins, centrosomal or otherwise, have been found to be inhibitors of ciliation. BCAP partially resembles OFD1, a known inhibitor of ciliogenesis, in that depletion of OFD1 modulates ciliogenesis in the same direction and with the same magnitude as depletion of BCAP (Tang et al., 2013). Whereas OFD1 has other roles in centrosome biology, we have so far not been able to determine other roles for BCAP in centrosome function. BCAPα appears to be present at centriolar satellites only in cycling cells with BCAPδ at the centrioles in addition; OFD1 is also present at the appendages (Singla et al., 2010). While super-resolution or immuno-gold TEM would categorically rule out other localisations, we do not observe any BCAPα at the centrioles in cycling cells, although we do observe BCAPδ at both the centrioles in addition to satellite staining.

The anti-BCAP antibody raised by Ponsard et al. was designed to detect all BCAP isoforms, using a mixture of peptide sequences encoded by exons 13 and 15. Exon 15 is included in all isoforms but exon 13 is present in only two of the long isoforms (L-BCAP/α and L-BCAP del 2/ε), and one short isoform (S-BCAP/η). Ponsard et al. also used human nasal epithelial (HNE) cells in an air-liquid interface culture to cause differentiation of the cells into multi-ciliated epithelial cells (Ponsard et al., 2007). Both the peptide against which the antibody was raised and the nature of the cell line used may contribute to the centrosome/centriole staining they observe, which resembles the staining we observe in some cells when GFP-BCAPδ is expressed in RPE-hTERT cells.

Another ciliation inhibitor, CP110, localises to the distal tips of centrioles to act as a capping protein (Schmidt et al., 2009). In this role, CP110 can control elongation of the pro-centrioles during centriole duplication in S-phase. BCAPα does not show centriolar localisation but BCAPδ does to some extent. During ciliogenesis, CP110 acts through Rab8 and Cep290 to control ciliation initiation (Tsang et al., 2008). Cep290 is another satellite protein. Whether BCAPα and/or BCAPδ link CP110 and Cep290 together or inhibit ciliogenesis by a different means would be a logical avenue for future investigation.

Any explanation of how BCAP controls ciliogenesis also has to consider the seven possible splice variants predicted by us and others. Our analysis in RPE-hTERT cells supports the presence of two protein isoforms, with only one detected by the anti-BCAP (Biorbyt) antibody but both detected by the Proteintech antibody. The BCAPα variant detected by the anti-BCAP (Biorbyt) antibody completely disappeared during ciliogenesis, implying its removal is required for ciliogenesis to initiate, continue and for cilia to be maintained. The anti-BCAP (Proteintech) antibody shows that total BCAP, i.e. the α and δ variants together, disappears at the start of ciliogenesis but returns, albeit at a lower levels, once ciliogenesis is complete. This can be explained if the δ variant also needs to be

Journal of Cell Science (2017) 130, 3360-3373 doi:10.1242/jcs.196642

removed for ciliogenesis to start and the δ form then has another function once cilia have been made. BCAP α and δ are partially redundant in that both can suppress ciliation but removal of either by RNAi only gives half the rate of ciliation compared with that observed when both are removed at the same time. In HNE cells, which differentiate into multi-ciliated (motile) cells, as opposed to monociliated (immotile) RPE-hTERT cells, more isoforms may be needed to ensure this process is properly controlled. An added complication in multi-ciliated cells is the requirement for centriole duplication in order to generate the (hundreds of) extra basal bodies, from which ciliogenesis then needs to be controlled and directed to the correct side of the cell.

We tested several other centrosome functions in BCAP-depleted cells as the siRNAs used for RNAi-mediated depletion target a region that is shared by both variants. Depletion of total BCAP, both α and δ variants, did not affect microtubule regrowth, cell polarity, migration or re-entry into the cell cycle.

Instead, the function of BCAPδ could be the regulation of cilium length. In cells transfected with siRNA duplexes that target both BCAP variants, cilium length is increased. Depletion of BCAPδ also results in an increase in cilium length but this is not observed when BCAPα is depleted. BCAPδ might, therefore, additionally act as a late inhibitor of ciliogenesis, moderating cilium length. There are, therefore, parallels and opposites to the roles ascribed to autophagy in ciliogenesis. In this regard it should be noticed that BCAP is predicted to have an APG6 domain (i.e. a region similar to that in the yeast autophagy protein 6, Fig. 2B).

Early on in response to serum starvation and initiation of ciliogenesis, autophagy is activated and Tang et al. (2013) have shown that this is needed to remove the ciliogenesis inhibitor OFD1. Pampliega et al. (2013) have further shown that autophagy needs to be directed differently before, during and after ciliogenesis. Once ciliation has finished, and full-length cilia have been made, autophagy is directed to limiting cilium length. In this situation, reduced autophagy results in abnormally long cilia. The latter mirrors the effect the absence of BCAP has in cells in which cilia had been established. Autophagy and BCAP both appear, therefore, to have a role in limiting cilium length at this stage. Pampliega et al. (2013) proposed that, in unciliated cells and those that possess cilia, autophagy is used to limit the availability of IFT20, which it turn affects Golgi–cilium movement. BCAP might, therefore, aid this process. However, when ciliogenesis initiates, BCAP needs to be removed. It is unclear then whether BCAP is a target of autophagy, like OFD1, or an aid in the pathway. The presence of two distinct isoforms might be due to this requirement, i.e. to have BCAP present before and after ciliogenesis but not during the process.

BCAP has also been shown to be upregulated in the mouse tracheal cell-ciliated model (Hoh et al., 2012), though the data do not show which variant (Tim Stearns, Departments of Biology and Genetics, Stanford University, Stanford, CA, personal communication). If BCAPδ is required to moderate cilium length, then it would be consistent that its expression is upregulated in cells with hundreds of cilia, as opposed to the one primary cilium in the cell lines studied here.

Future work is needed to place BCAP within known ciliogenesis regulatory networks, inhibitory mechanisms and processes that relieve this repression. Obvious processes to check are the autophagy pathway and IFT20-mediated control of primary ciliary vesicle formation. The CP110–Cep97–Cep290 pathway could be checked as well, though the current localisation data point away from this mechanism. These hypotheses will form the basis of more-extensive future studies.

MATERIALS AND METHODS

Cell culture

HeLa cells were provided by Prof. George Dickson's laboratory at Royal Holloway. The human telomerase reverse transcriptase immortalised human retinal pigment epithelial cell line (hTERT RPE-1, ATCC catalog no: CRL-4000; here referred to as RPE1-hTERT) was kindly provided by Prof. Erich Nigg, Basel, Switzerland. HeLa cells were grown in Dulbecco's modified Eagle's medium (Sigma D6546) supplemented with 2 mM L-Glutamine (Sigma G7513), 10% foetal bovine serum (FBS; Gibco 10500-064) and 1% antibiotic-antimycotic mixture (Gibco 15140-122). hTERT-RPE-1 cells were grown in DMEM with nutrient mixture F-12 Ham (Sigma D6421) supplemented with 10% FBS, 0.348% sodium bicarbonate and 1% antibiotic-antimycotic mixture. HuH-7 cells were cultured in DMEM (Sigma D6546) supplemented with 10% FBS and 1% antibiotic-antimycotic mixture. Cells were grown in Corning 25 and 75 cm^2 vent-capped flasks and 6-well plates (Nunc, Denmark) and incubated at 37°C with 5% CO_2 in a humidified incubator and confluence was assessed by microscopy. Ethanol-washed coverslips were added to the 6-well plates to enable subsequent processing for immunofluorescence microscopy. These coverslips were fixed in methanol at −20°C or 4% (v/v) formaldehyde (FA) for 3-5 min before antibody incubation.

Immunocytochemistry

Coverslips were blocked in 1% or 3% BSA in PBS for 30 min at room temperature. After blocking, coverslips were placed on top of a paraffin film attached to flat surface. Then 100–200 µl of primary antibody solution was added to the top of the coverslip. The coverslip were incubated with the primary antibody for 60–120 min at room temperature or overnight at 4°C. After the incubation, coverslips were transferred back to a 6-well plate and washed three times with PBS at room temperature. Then the coverslips were incubated with the secondary antibodies identically to the procedure described above and incubated for 60 min at room temperature. After the incubation, coverslips were transferred back to a 6-well plate and washed again with PBS three times and then mounted on 10–15 µl of Vectashield mounting medium with DAPI (Vectorlabs, Peterborough, UK) onto glass slides for microscopy. The mounted coverslips were sealed with nail varnish and left to dry for 1–2 h in a dark chamber before microscopy. Primary antibodies were used as follows: mouse acetylated α-tubulin (Sigma-Aldrich, T7451; 1:500), mouse anti-γ-tubulin (Sigma-Aldrich, T6557; 1:2500), mouse anti-PCM1 (CL0206, Sigma; 1:1000), rabbit anti-γ-tubulin (Sigma-Aldrich, T5192; 1:1000), mouse anti-golgin-97 (ThermoFisher, Q92805; 1:1000), rabbit anti- BCAP (Biorbyt, orb31049; 1:100), rabbit anti- BCAP (Proteintech, 23887-1-AP), and rabbit anti-PCM-1 (Sigma, HPA23374; 1:1000). Secondary antibodies were used as follows: anti-mouse Alexa Fluor 594and anti-rabbit Alexa Fluor 488 (both Invitrogen; 1:1000).

Images were collected using a Nikon Eclipse TE300 inverted microscope (Nikon, UK) with either a 40× Plan Fluor objective (Nikon) or a 60× Plan Apochromat oil immersion objective with NA 1.4 standard filter sets (Nikon) attached to a 1.3 megapixel ORCA-100 cooled CCD camera (model C4742-95, Hamamatsu, Japan), with Hamamatsu HCImageLive (Hamamatsu Corporation, Japan) software or using a Nikon Eclipse Ni-E microscope (CF160 optical system, Nikon) with a 60× Plan Apochromat oil immersion objective attached to a 1.5 megapixel monochrome DS-Qi1MC cooled CCD camera and NIE Br (Nikon, UK) software. Confocal microscopy stacks were obtained by using the Olympus IX81/FV-1000 laser confocal system with a 63× Plan Apochromat oil immersion objective (Olympus) using an Ar gas laser and a He–Ne diode laser. Image *Z*-stacks were analysed by using Olympus FV-1000 Fluoview 2.0 C software.

Molecular cloning and transient transfection of DNA into mammalian cells

Molecular cloning followed standard protocols (Sambrook and Russell, 2001) and the manufacturer's instructions of the of the kits, reagents and enzymes used. All restriction enzymes and polymerases were obtained from Promega (UK). The mouse full-length BCAP cDNA I.M.A.G.E clone (cDNA clone MGC: 28123, IMAGE:3979963, GenBank accession no.: BC020075.1, Gene ID 52184) was purchased from Source BioScience (Nottingham, UK). The mouse cDNA was amplified and 5′ *Bam*H I and 3′

Xho I restriction sites were added to the cDNA during amplification by PCR using (5′-ttttggatcctcATGGAGATGCCTACTAGTGATGG-3′ and 5′-ttttc-tcgagttagtcgacTCTAAACATCGTTACATAGGAAATTTG-3′). Then a *Bam*HI- *Xho*I fragment containing full-length BCAP was inserted into pCS2P+EGFPN digested with *Xho*I and *Bgl*II. Similarly, hBCAPα and hBCAPδ were cloned using primers 5′-tttgggatcctgATGGAGAAGGCT-GTAAATGA-3′ (forward primer for both transcripts), 5′-tttgtcgacTCATGGAGTCTCTGGATCAC-3′ (reverse primer hBCAPα) and 5′-tttgtcgacTTATTCAAACATTGTTACATAA-3′ (reverse primer hBCAPδ); lower case letters indicate non-homologous DNA, including restriction sites. The PCR product was cut with *Bam*H I−*Sal*1 and inserted into pCS2P+EGFPN cut with *Sal*1−*Bgl* II.

HeLa and RPE1-hTERT cells were transiently transfected with DNA constructs for expression using Lipofectamine 2000 (Life Technologies) according to the manufacturer's protocols. For all the transfections in 6-well format, 2.5–3 µg of plasmid DNA was used and diluted in 250 µl Opti-MEM. Lipofectamine 2000 and DNA mixtures were separately incubated for 5-10 min at room temperature before combining and adding to each well. Cells were then incubated for 5-6 h before the medium was replaced with serum-supplemented antibiotic-free medium and then incubated for a further 24-48 h.

RNA interference

The small interfering RNAs (siRNAs) were designed with custom RNA synthesis tools (siDESIGN Center) provided by GE Dharmacon to BCAP transcripts: XM_005271056, NM_001184766, NM_020729, XM_005271057, NM_001184765, NM_001007022, XM_005271055, XM_005271054. The siRNA oligonucleotide sequences were designed to have an overlap of 19 nucleotides and two nucleotide overhangs on both 3′-end of the sense and anti-sense strands. The following siRNAs were used for the experiments: Hs*BCAP* siRNA1 5′-GCAAGAAGCAGCUGAAA-UAUU-3′ (sense) 5′-GCAAGAAGCAGCUGAAAUAUU-3′ (antisense) and Hs*BCAP* siRNA2, 5′-GGAGAAGGCUGUAAAUGAUUU-3′ (sense), 5′-AUCAUUUACAGCCUUCUCCUU-3′ (antisense). The siRNA sequences targeting the two individual transcripts Hs*BCAP*α siRNA 5′-UGAAGGAGUUAGAGCGUGUUU-3′ (sense), 5′-ACACGCUCUAAC-UCCUUCAUU-3′ (antisense) and Hs*BCAP* δ siRNA 5′-AGUCUUGAG-AAGUCGGAAAUU-3′ (sense), 5′-UUUCCGACUUCUCAAGACUUU-3′ (antisense). A SMARTPool ON-TARGETplus siRNA to PCM-1 was purchased from Dharmacon. Oligonucleotides were resuspended in 200 µl of RNase-free H_2O to make a stock solution of 100 µM and stored at −80°C. The working concentrations of 10 µM aliquots were also made by diluting 100 µM stock with RNase free water and stored in −80°C. For delivering siRNAs to mammalian cells, Lipofectamine RNAiMAX (Life Technologies) was used according to manufacturer's protocol. For transfection of mammalian cell lines, 1×10^6 cells were plated per well of a 6-well plate (reverse transfection). All the transfection complexes were prepared in sterile 6-well plates and for each well, 2.5−3 µl of siRNA (from 10 µM working concentration) and 7.5 µl of Lipofectamine RNAiMAX diluted in 500 µl of Opti-MEM and mixtures were incubated at room temperature for 10−15 min to allow the complexes to form. Then, the cell suspension was added to each well containing siRNA-RNAiMAX complexes and diluted with culture medium without antibiotics to make a final volume of 2.5 ml per well.

Cell extracts, SDS-PAGE and western blotting

Whole-cell extracts for western blotting were prepared by washing cells in phosphate-buffered saline (PBS), followed by lysis in cell lysis buffer (50 mM Tris-HCL pH 7.5, 150 mM NaCl, 1 mM EDTA, 10% glycerol, 1% Triton X-100) containing a protease inhibitor cocktail (P8340, Sigma-Aldrich) at 4°C for 30 min. Then the cell debris was removed by centrifuging at 12,000 ***g*** at 4°C for 20 min. Prior to SDS-PAGE, protein concentration was determined using a BioRad DC assay (BioRad, UK) according to the manufacturer's instructions. Small 10% SDS polyacrylamide gels (8×6.5 cm) with 0.75 mm thickness were hand cast using a Biorad Mini-Protein II casting chamber. Approximately 5−15 µg of protein samples were prepared with 1× SDS-PAGE buffer and 1× reducing agent (Invitrogen), heat-denatured for 10 min at 70°C and kept in ice until loading. 20 µl of the protein sample alone with PageRuler Plus pre-stained protein ladder (ThermoFisher Scientific) were loaded into each well and gels were run with SDS-PAGE running buffer (Sambrook and Russell, 2001) in a BioRad Mini Protein II gel chamber at 100 V for 1.5 h. The proteins separated from SDS-PAGE gel were subsequently transferred onto activated PVDF-FL (Millipore) membrane with an aid of BioRad Mini-Protean II wet blotting system filled with transfer buffer. Membranes were blocked with Odyssey blocking solution (Licor) or 1× casein buffer (Sigma-Aldrich, B6429), and washed with Tris-buffered saline containing 0.5% Tween20 (Sigma-Aldrich) and probed with primary antibodies. Bound primary antibodies were detected using secondary antibodies (anti-mouse IRDye 680RD, 1:15,000 and anti-rabbit IRDye 800CW, 1:15000) using Odyssey SA near infrared fluorescent (Licor) detector. Images were captured using Image studio software (Licor) version 3.

Cell migration assay (scratch-wound assay)

To assess the cell migration pattern and polarity, a scratch-wound assay was performed on RPE1-hTERTcells. The cells were seeded on to a glass coverslip placed in a 6-well plate and grown in an incubator to reach about 90% confluency. Then a linear scratch wound was made using a blunt sterile P200 tip between parallel edges of the coverslip as described in Wells and Parsons (2011) and Nobes and Hall (1999). The coverslips were washed two times with PBS and incubated with fresh medium for 24 h until the wound was closed. The coverslips were fixed in cold methanol at different time points before processing for immunocytochemistry as above.

Cell cycle synchronisation

For cell synchronisation at G2/M transition phase, hTERT-RPE1 cells were seeded and cultured until 70−80% confluency followed by treatment with 1.5 µM nocodozole for 24 h as described (Uetake and Sluder, 2007). To release from G2/M arrest, cells were washed twice with PBS and incubated in serum free growth medium. Cells were fixed at various time points in 1% FA and stained with anti-γ-tubulin, anti-BCAP and anti-acetylated α-tubulin primary antibodies as above.

Cell cycle analysis using FACS

For the FACS based cell cycle analysis, hTERT-RPE-1 cells were grown under normal culture conditions in a 6-well plate. Once the cells reached 80−90% confluency, cells were trypsinised and harvested as described above and washed twice with PBS. The cells were then fixed in ice-cold 70% ethanol for at least 30 min on ice and washed twice with PBS. Cells were treated with 100 µg/ml RNase A solution in PBS followed by 50 µg/ml propidium iodide (PI). Cells were stained overnight in a dark chamber at room temperature and data were collected using a BD FACSCANTO I (BD Bioscience, Oxford, UK) flow cytometer set to collect in the linear scale. Cell cycle analysis was performed using BD FACSDiva (BD Bioscience) and FlowJo version X.

Phylogenetic analysis

Data were aligned and trees were constructed in CLC genomics workbench v7.5, using the default settings for alignment (Gap open cost 10, Gap extension cost 1) and with trees estimated using Kimura protein distances, with neighbour joining.

Acknowledgements

We would like to thank Simona Ursu for technical support. We thank Prof. Ian Barnes and Dr Selina Brace (NHM, London) for their assistance in generating the phylogenetic tree.

Competing interests

The authors declare no competing or financial interests.

Author contributions

Conceptualization: C.J.W.; Validation: A.I.; Formal analysis: P.d.S., A.I.; Investigation: P.d.S., A.I.; Writing - original draft: A.I., C.J.W.; Writing - review & editing: J.N.M., C.J.W.; Supervision: J.N.M., C.J.W.; Project administration: J.N.M., C.J.W.

Funding

This research was funded by the Royal Society [grant number: RG 2009/R1].

Supplementary information

Supplementary information available online at
http://jcs.biologists.org/lookup/doi/10.1242/jcs.196642.supplemental

References

Ansley, S. J., Badano, J. L., Blacque, O. E., Hill, J., Hoskins, B. E., Leitch, C. C., Kim, J. C., Ross, A. J., Eichers, E. R., Teslovich, T. M. et al. (2003). Basal body dysfunction is a likely cause of pleiotropic Bardet-Biedl syndrome. *Nature* **425**, 628-633.

Badano, J. L., Mitsuma, N., Beales, P. L. and Katsanis, N. (2006). The ciliopathies: an emerging class of human genetic disorders. *Annu. Rev. Genomics Hum. Genet.* **7**, 125-148.

Balczon, R., Bao, L. and Zimmer, W. E. (1994). PCM-1, A 228-kD centrosome autoantigen with a distinct cell cycle distribution. *J. Cell Biol.* **124**, 783-793.

Basto, R., Lau, J., Vinogradova, T., Gardiol, A., Woods, C. G., Khodjakov, A. and Raff, J. W. (2006). Flies without centrioles. *Cell* **125**, 1375-1386.

Bornens, M. (2002). Centrosome composition and microtubule anchoring mechanisms. *Curr. Opin. Cell Biol.* **14**, 25-34.

Collin, G. B., Marshall, J. D., Ikeda, A., So, W. V., Russell-Eggitt, I., Maffei, P., Beck, S., Boerkoel, C. F., Sicolo, N., Martin, M. et al. (2002). Mutations in ALMS1 cause obesity, type 2 diabetes and neurosensory degeneration in Alstrom syndrome. *Nat. Genet.* **31**, 74-78.

Dawe, H. R., Smith, U. M., Cullinane, A. R., Gerrelli, D., Cox, P., Badano, J. L., Blair-Reid, S., Sriram, N., Katsanis, N., Attie-Bitach, T. et al. (2007). The Meckel-Gruber Syndrome proteins MKS1 and meckelin interact and are required for primary cilium formation. *Hum. Mol. Genet.* **16**, 173-186.

Doxsey, S. (2001). Re-evaluating centrosome function. *Nat. Rev. Mol. Cell Biol.* **2**, 688-698.

Ferrante, M. I., Romio, L., Castro, S., Collins, J. E., Goulding, D. A., Stemple, D. L., Woolf, A. S. and Wilson, S. W. (2009). Convergent extension movements and ciliary function are mediated by ofd1, a zebrafish orthologue of the human oral-facial-digital type 1 syndrome gene. *Hum. Mol. Genet.* **18**, 289-303.

Fry, A. M., Meraldi, P. and Nigg, E. A. (1998). A centrosomal function for the human Nek2 protein kinase, a member of the NIMA family of cell cycle regulators. *EMBO J.* **17**, 470-481.

Hoh, R. A., Stowe, T. R., Turk, E. and Stearns, T. (2012). Transcriptional program of ciliated epithelial cells reveals new cilium and centrosome components and links to human disease. *PLoS One* **7**, e52166.

Huangfu, D., Liu, A., Rakeman, A. S., Murcia, N. S., Niswander, L. and Anderson, K. V. (2003). Hedgehog signalling in the mouse requires intraflagellar transport proteins. *Nature* **426**, 83-87.

Kasahara, K., Kawakami, Y., Kiyono, T., Yonemura, S., Kawamura, Y., Era, S., Matsuzaki, F., Goshima, N. and Inagaki, M. (2014). Ubiquitin-proteasome system controls ciliogenesis at the initial step of axoneme extension. *Nat. Commun.* **5**, 5081.

Kim, J., Lee, J. E., Heynen-Genel, S., Suyama, E., Ono, K., Lee, K. Y., Ideker, T., Aza-Blanc, P. and Gleeson, J. G. (2010). Functional genomic screen for modulators of ciliogenesis and cilium length. *Nature* **464**, 1048-1051.

Kubo, A., Sasaki, H., Yuba-Kubo, A., Tsukita, S. and Shiina, N. (1999). Centriolar satellites: molecular characterization, ATP-dependent movement toward centrioles and possible involvement in ciliogenesis. *J. Cell Biol.* **147**, 969-980.

Lange, B. M. and Gull, K. (1995). A molecular marker for centriole maturation in the mammalian cell cycle. *J. Cell Biol.* **130**, 919-927.

Luxton, G. W. G. and Gundersen, G. G. (2011). Orientation and function of the nuclear-centrosomal axis during cell migration. *Curr. Opin. Cell Biol.* **23**, 579-588.

Mikule, K., Delaval, B., Kaldis, P., Jurcyzk, A., Hergert, P. and Doxsey, S. (2007). Loss of centrosome integrity induces p38-p53-p21-dependent G1-S arrest. *Nat. Cell Biol.* **2**, 160-170.

Mogensen, M. M., Malik, A., Piel, M., Bouckson-Castaing, V. and Bornens, M. (2000). Microtubule minus-end anchorage at centrosomal and non-centrosomal sites: the role of ninein. *J. Cell Sci.* **113**, 3013-3023.

Nakagawa, Y., Yamane, Y., Okanoue, T., Tsukita, S. and Tsukita, S. (2001). Outer dense fiber 2 is a widespread centrosome scaffold component preferentially associated with mother centrioles: its identification from isolated centrosomes. *Mol. Biol. Cell* **12**, 1687-1697.

Nigg, E. A. and Raff, J. W. (2009). Centrioles, centrosomes, and cilia in health and disease. *Cell* **139**, 663-678.

Nobes, C. D. and Hall, A. (1999). Rho GTPases control polarity, protrusion, and adhesion during cell movement. *J. Cell Biol.* **144**, 1235-1244.

Novorol, C., Burkhardt, J., Wood, K. J., Iqbal, A., Roque, C., Coutts, N., Almeida, A. D., He, J., Wilkinson, C. J. and Harris, W. A. (2013). Microcephaly models in the developing zebrafish retinal neuroepithelium point to an underlying defect in metaphase progression. *Open Biol.* **3**, 130065.

Ong, A. C. M. and Wheatley, D. N. (2003). Polycystic kidney disease–the ciliary connection. *Lancet* **361**, 774-776.

Pampliega, O., Orhon, I., Patel, B., Sridhar, S., Díaz-Carretero, A., Beau, I., Codogno, P., Satir, B. H., Satir, P. and Cuervo, A. M. (2013). Functional interaction between autophagy and ciliogenesis. *Nature* **502**, 194-200.

Ponsard, C., Seltzer, V., Perret, E., Tournier, F. and Middendorp, S. (2007). Identification of BCAP, a new protein associated with basal bodies and centrioles. *Front. Biosci.* **12**, 3683-3693.

Sambrook, J. and Russell, D. (2001). *Molecular Cloning: A Laboratory Manual*. New York: Cold Spring Harbor Laboratory Press.

Satir, P. and Christensen, S. T. (2007). Overview of structure and function of mammalian cilia. *Annu. Rev. Physiol.* **69**, 377-400.

Schmidt, T. I., Kleylein-Sohn, J., Westendorf, J., Le Clech, M., Lavoie, S. B., Stierhof, Y.-D. and Nigg, E. A. (2009). Control of centriole length by CPAP and CP110. *Curr. Biol.* **19**, 1005-1011.

Singla, V., Romaguera-Ros, M., Garcia-Verdugo, J. M. and Reiter, J. F. (2010). Ofd1, a human disease gene, regulates the length and distal structure of centrioles. *Dev. Cell* **18**, 410-424.

Sorokin, S. (1962). Centrioles and the formation of rudimentary cilia by fibroblasts and smooth muscle cells. *J. Cell Biol.* **15**, 363-377.

Stevens, N. R., Raposo, A. A., Basto, R., St Johnston, D. and Raff, J. W. (2007). From stem cell to embryo without centrioles. *Curr. Biol.* **17**, 1498-1503.

Stowe, T. R., Wilkinson, C. J., Iqbal, A. and Stearns, T. (2012). The centriolar satellite proteins Cep72 and Cep290 interact and are required for recruitment of BBS proteins to the cilium. *Mol. Biol. Cell* **23**, 3322-3335.

Tang, Z., Lin, M. G., Stowe, T. R., Chen, S., Zhu, M., Stearns, T., Franco, B. and Zhong, Q. (2013). Autophagy promotes primary ciliogenesis by removing OFD1 from centriolar satellites. *Nature* **502**, 254-257.

Tassin, A.-M. and Bornens, M. (1999). Centrosome structure and microtubule nucleation in animal cells. *Biol. Cell* **91**, 343-354.

Tollenaere, M. A. X., Mailand, N. and Bekker-Jensen, S. (2015). Centriolar satellites: key mediators of centrosome functions. *Cell. Mol. Life Sci.* **72**, 11-23.

Tsang, W. Y., Bossard, C., Khanna, H., Peränen, J., Swaroop, A., Malhotra, V. and Dynlacht, B. D. (2008). CP110 suppresses primary cilia formation through its interaction with CEP290, a protein deficient in human ciliary disease. *Dev. Cell* **15**, 187-197.

Uetake, Y. and Sluder, G. (2007). Cell-cycle progression without an intact microtuble cytoskeleton. *Curr. Biol.* **17**, 2081-2086.

Wells, C. M. and Parsons, M. (2011). *Cell Migration: Developmental Methods and Protocols*. New York: Humana Press; Springer.